Linear Suppression of Intercarrier Interference in Time-Varying OFDM Systems: From the Viewpoint of Multiuser Detection

Husheng Li

Abstract: **Intercarrier interference (ICI) in orthogonal frequency division multiplexing (OFDM) systems, which causes substantial performance degradation in time-varying fading channels, is analyzed. An equivalent spreading code formulation is derived based on the analogy of OFDM and code division multiple access (CDMA) systems. Techniques as linear multiuser detection in CDMA systems are applied to suppress the ICI in OFDM systems. The performance of linear detection, measured using multiuser efficiency and asymptotic multiuser efficiency, is analyzed given the assumption of perfect channel state information (CSI), which serves as an upper bound for the performance of practical systems. For systems without CSI, time domain and frequency domain channel estimation based linear detectors are proposed. The performance gains and robustness of a linear minimum mean square error (LMMSE) filter over a traditional filter (TF) and matched filter (MF) in the high signal-to-noise ratio (SNR) regime are demonstrated with numerical simulation results.**

Index Terms: **Intercarrier interference (ICI), multiuser detection, orthogonal frequency division multiplexing (OFDM).**

I. INTRODUCTION

Orthogonal frequency division multiplexing (OFDM) is becoming a fundamental signaling technique for the new generation of wireless communication systems, which are characterized by high speed and reliable data transmission, e.g., ultra mobile wideband (UMB) developed by the 3rd generation partnership project 2 (3GPP2), long term evolution (LTE) developed by the 3rd generation partnership project (3GPP) and worldwide interoperability for microwave access (WiMAX, equivalently IEEE 802.16). One of the advantages of OFDM is that different data streams are transmitted on different subcarriers, thus achieving orthogonality and avoiding interference across different data streams. However, the orthogonal transmission is achieved only in ideal situations. In practical systems, there exists intercarrier interference (ICI) which is caused by Doppler spread [1], [2], frequency carrier offset [3], [4], or time synchronization errors [5]. ICI can substantially impair the system performance, particularly in the high signal-to-noise ratio (SNR) regime since system performance is interference limited in such scenarios. Meanwhile, the power of a data stream is also dispersed to other subcarriers and a portion of the power is wasted if only the desired subcarrier is used for detection. A variety of algorithms have been proposed to mitigate the ICI in OFDM systems. In [1], a linear filter is used to suppress the ICI caused by Doppler shift in multiple-input multiple-output (MIMO) OFDM systems, while a piecewise linear approximation is used to combat the same ICI in single antenna systems in [2]. For ICI caused by frequency offset, self interference cancellation is adopted in [3]; and the frequency offset can also be estimated explicitly, thus removing the corresponding ICI [6]. In [5], the sensitivity of the channel estimator is exploited to improve the performance of time synchronization, thus alleviating the ICI incurred by a time synchronization error.

In this paper, we focus on the ICI caused by Doppler shift since it exists in all time-varying (or equivalently, time-selective) channels, particularly in high mobility situations. As mentioned before, this problem has been addressed in [1] and [2]. However, we tackle this problem from the viewpoint of multiuser detection [7], which is originated from multiuser detection in code division multiple-access (CDMA) systems, since the ICI and different data streams can be regarded as multiple-access interference (MAI) and different users in CDMA systems, respectively. Similarly, the vector output of a data stream, namely the output over all subcarriers, can be considered as its spreading code, although it is different from conventional binary spreading codes used in CDMA systems. Then, the OFDM system can be converted into a CDMA system. The advantage of such a strategy is that the algorithms and corresponding performance analysis developed in the community of multiuser detection can be directly applied to the ICI mitigation problem. It also demonstrates that the technique of multiuser detection is not confined to CDMA systems.

In CDMA systems, it has been demonstrated that optimal multiuser detection can considerably suppress the MAI and improve the output signal-to-interference-plus-noise ratio (SINR) compared with a matched filter (MF) [7]–[9]. In particular, the SINR tends to infinity as the noise power vanishes, which implies that the multiuser detection-based CDMA system is not interference limited. However, the optimal multiuser detection incurs computational cost exponentially increasing with the number of users, which is infeasible for practical systems since there exist many users within a typical cell. Therefore, low-complexity algorithms have been considered for implementation at the cost of tolerable performance degradation. For example, linear minimum mean square error (LMMSE) multiuser detection was proposed in [10] and has been demonstrated to achieve good performance [11]. For nonlinear processing, parallel interference cancelation (PIC) [12] and successive interference cancelation (SIC) [13] have been adopted to cancel the MAI using

Manuscript received March 15, 2008; approved for publication by Lee Garth, Division II Editor, October 16, 2010.

H. Li is with the Department of Electrical Engineering and Computer Science, the University of Tennessee, Knoxville, TN, 37996, email: husheng@ece.utk.edu.

feedback, particularly when channel coding is used. In the community of multiuser detection, multiuser efficiency (ME) is used to measure how close the output SINR of a multiuser detector is to that of the single user case, and the asymptotic multiuser efficiency (AME) is used to evaluate the efficiency of interference mitigation in the high SNR regime [7].

In this paper, we consider low-complexity algorithms without the aid of channel codes. It is interesting to consider the performance of channel codes; however, it is beyond the scope of this paper. Therefore, we adopt linear detectors to suppress the ICI after formulating the spreading codes of all data streams, based on the assumption that perfect channel state information (CSI) is known. Three linear detectors, the traditional filter (TF), MF, and LMMSE detector, are derived, analyzed and compared. Analytical methods from multiuser detection are used to analyze the performance of these detectors, such as the ME and AME. For practical systems, we analyze the performance with imperfect channel estimation and propose an algorithm for estimating truncated spreading codes in the frequency domain. Numerical results demonstrate that the LMMSE detector achieves the best performance among these three detectors in the high SNR regime.

The remainder of this paper is organized as follows. The time-varying system model of OFDM is introduced in Section II. In Section III, the OFDM system is converted into a CDMA system and the expression for the corresponding spread code is provided. Based on the equivalent CDMA system, three linear detectors are derived. In Section IV, the performance of these three detectors is analyzed for frequency flat and frequency selective fading channels, respectively, given the assumption of perfect CSI. In Section V, we consider systems with channel estimation in the time and frequency domains, respectively. Numerical results and conclusions are provided in Sections VI and VII.

Below is some mathematical notation used in this paper:

- $\mathbf{x}^H$ is the conjugate transpose of the vector $\mathbf{x}$.
- $\mathrm{mod}(i,j)$ denotes the modulus of i with respect to j.
- $E\{X\}$ denotes the expectation of the random variable X.
- $\mathrm{Re}(x)$ means the real part of complex number x.

II. SYSTEM MODEL

We consider an OFDM system using N subcarriers. For simplicity, we assume perfect synchronization and consider only baseband signals. On denoting the information symbols[1] on the N subcarriers by $\{X_k\}_{k=0,\cdots,N-1}$, which are assumed to have power $|X_k|^2 = N$, the corresponding time domain chip sequence within one OFDM symbol period is the output of the inverse discrete Fourier transform (IDFT) of $\{\mathbf{X}_k\}_{k=0,\cdots,N-1}$, which is given by

$$x_m = \frac{1}{N}\sum_{k=0}^{N-1} X_k w^{mk}, \quad m = 0,\cdots,N-1 \tag{1}$$

where $w \triangleq e^{\frac{j2\pi}{N}}$. To combat the possible time dispersion of the channel, a sufficiently long cyclic prefix is added in front of the time domain chips in (1).

[1] In this paper, an information symbol means the symbol of each data stream sent over each subcarrier; an OFDM symbol includes all information symbols simultaneously.

We assume that the OFDM system operates over a time-varying multipath channel with L resolvable paths, each being represented by a random process of channel gains. We denote the sample paths of the channel gains within one OFDM symbol period by $\{h_m^{(l)}\}_{l=0,\cdots,L-1,\, m=0,\cdots,N-1}$ where $h_m^{(l)}$ represents the channel gain of path l during chip period m, and $\{\tau_l\}_{l=0,\cdots,L-1}$ represent the path delays with convention $\tau_0 = 0$. Also, we denote the average channel gain, namely $\frac{1}{N}\sum_{m=0}^{N-1} h_m^{(l)}$, by $\bar{h}^{(l)}$.

We denote the corresponding channel power gains by $\{g_m^{(l)}\}_{l=0,\cdots,L-1,\, m=0,\cdots,N-1}$ where $g_m^{(l)} = |h_m^{(l)}|^2$. We denote the average channel power gain of the lth path, namely $\frac{1}{N}\sum_{m=0}^{N-1} g_m^{(l)}$ by $\bar{g}^{(l)}$. We also define the variation of channel power gain

$$\delta g_m^{(l)} \triangleq g_m^{(l)} - \bar{g}^{(l)} \tag{2}$$

and normalized variance

$$\sigma_g^2(l) \triangleq \frac{1}{N}\sum_{m=0}^{N-1}\left(\delta g_m^{(l)}\right)^2. \tag{3}$$

Similarly, we define the variance of the channel gains, which is given by

$$\sigma_h^2(l) \triangleq \bar{g}^l - \left|\bar{h}^{(l)}\right|^2. \tag{4}$$

On assuming that there is no inter-chip interference for each path and the cyclic prefix period is longer than the largest path delay, the channel output is given by

$$y_m = \sum_{l=0}^{L-1} x_{\mathrm{mod}(m-\tau_l,N)} h_m^{(l)} + n_m, \quad m = 0,\cdots,N-1 \tag{5}$$

where n_m is complex additive white Gaussian noise with variance σ_n^2. Then the time domain output is transformed to the frequency domain by carrying out the discrete Fourier transform (DFT), which is given by

$$Y_k = \sum_{m=0}^{N-1} y_m w^{-mk} + W_k, \quad k = 0,\cdots,N-1 \tag{6}$$

where W_k is the DFT of the noise sequence $\{n_m\}_{m=0,\cdots,N-1}$ whose variance is given by $N\sigma_n^2$.

By applying the property for the DFT, that multiplication in the time domain is equivalent to circular convolution (denoted by $\star$) in the frequency domain, we can obtain the frequency domain output directly, which is given by

$$\mathbf{Y} = \frac{1}{N}\sum_{l=0}^{L-1} \mathbf{H}^{(l)} \star \mathbf{X}^{(l)} + \mathbf{W} \tag{7}$$

where $\mathbf{Y} \triangleq (Y_0\ Y_1\ \cdots\ Y_{N-1})^T$, $\mathbf{H}^{(l)} \triangleq (H_0^{(l)}\ H_1^{(l)}\ \cdots\ H_{N-1}^{(l)})^T$, $\mathbf{X}^{(l)} \triangleq (X_0\ \ X_1 w^{-\tau_l}\ \ \cdots\ \ X_{N-1} w^{-\tau_l(N-1)})^T$, and $\mathbf{W} \triangleq (W_0\ W_1\ \cdots\ W_{N-1})^T$.

Note that $\mathbf{H}^{(l)}$ is the DFT of the channel gain sequence $\{h_m^{(l)}\}_{m=0,\cdots,N-1}$ and the expression for $\mathbf{X}^{(l)}$ stems from the time domain shift property of the DFT. For the kth element, (7) can be rewritten as

$$Y_k = \frac{1}{N}\sum_{l=0}^{L-1}\sum_{p=0}^{N-1} H_p^{(l)} X_{\mathrm{mod}(k-p,N)} w^{-\tau_l(k-p)} + W_k. \quad (8)$$

From (8), we can see that the frequency domain output Y_k is impacted by all $\{X_n\}_{n=0,\cdots,N-1}$ if $H_p^{(l)} \neq 0$. We call the interference from symbol X_n on Y_k, $n \neq k$, ICI. It is easy to observe that the ICI equals zero if and only if, $\forall l = 0, \cdots, L-1$, $H_p^{(l)} = 0$ when $p > 0$, which is equivalent to that $h_m^{(l)}$ is a constant and the channel is thus time-invariant. Therefore, the intercarrier interference stems from the time selectivity of the channel gains and is then dual to the intersymbol interference (ISI) in then time domain caused by frequency selectivity.

III. LINEAR MULTIUSER DETECTION

In this section, we introduce three types of linear detectors for the detection of OFDM symbols, whose information symbol output on subcarrier k is given by

$$z_k = \mathbf{v}_k^H \mathbf{Y} \quad (9)$$

where the column vector $\mathbf{v}_k$ is the linear detector for subcarrier k. We first translate the detection of OFDM symbols into a CDMA-like multiuser formulation and then introduce known multiuser detection results.

A. Multiuser Formulation

As explained in the introduction, we can regard each symbol X_k, $k = 0, \cdots, N-1$, in (7) as a virtual user. Then, the virtual users transmit over an N-vector space and we define the column vector output of virtual user k (assuming $X_1 = 1$), denoted by $\mathbf{s}_k$, as its *spreading code* (here, we adopt the terminology of CDMA systems). According to (8), the spreading code matrix $\mathbf{S} \triangleq (\mathbf{s}_1, \cdots, \mathbf{s}_N)$ is given by

$$\mathbf{S} = \frac{1}{N} \times \begin{pmatrix} \sum_{l=0}^{L-1} H_0^{(l)} & \sum_{l=0}^{L-1} H_{N-1}^{(l)} w^{-\tau_l} & \cdots & \sum_{l=0}^{L-1} H_1^{(l)} w^{-\tau_l(N-1)} \\ \sum_{l=0}^{L-1} H_1^{(l)} & \sum_{l=0}^{L-1} H_0^{(l)} w^{-\tau_l} & \cdots & \sum_{l=0}^{L-1} H_2^{(l)} w^{-\tau_l(N-1)} \\ \vdots & \vdots & \ddots & \vdots \\ \sum_{l=0}^{L-1} H_{N-1}^{(l)} & \sum_{l=0}^{L-1} H_{N-2}^{(l)} w^{-\tau_l} & \cdots & \sum_{l=0}^{L-1} H_0^{(l)} w^{-\tau_l(N-1)} \end{pmatrix} \quad (10)$$

or equivalently

$$(\mathbf{S})_{pq} = \frac{1}{N}\sum_{l=0}^{L-1} H_{\mathrm{mod}(p-q,N)}^{(l)} w^{-\tau_l q}, \quad (11)$$
$$p = 0, \cdots, N-1, \quad q = 0, \cdots, N-1.$$

Thus, we convert the OFDM system into an equivalent CDMA system with spreading gain N and N active users, in which the received signal is given by

$$\mathbf{Y} = \sum_{k=0}^{N-1} \mathbf{s}_k X_k + \mathbf{W} \quad (12)$$

or equivalently

$$\mathbf{Y} = \mathbf{S}\mathbf{X} + \mathbf{W}. \quad (13)$$

The equivalent CDMA system and the traditional CDMA system (we assume using random spreading code) differ in the following respects:

- The spreading code elements in the equivalent CDMA system are correlated while those in a traditional CDMA system are mutually independent. This difference implies that we cannot apply the theory of random matrices, which is very useful in analyzing traditional CDMA systems.
- In the ideal case, only one element in a spreading code in the equivalent CDMA system is non-zero while the spreading code of a traditional CDMA system spreads over all dimensions.
- The spreading codes of different virtual users are always synchronous in the equivalent CDMA system while they could be asynchronous in a traditional CDMA system.
- The equivalent CDMA system spreads in the frequency domain while the traditional CDMA system spreads in the time domain.
- In the equivalent CDMA system, the system load, defined as the ratio between the number of active users and the spreading gain, is always 1 while it is an arbitrary positive number in a traditional CDMA system.

B. Multiuser Detectors

We consider the following linear multiuser detectors for the equivalent CDMA system.

B.1 Traditional Filter

In a traditional OFDM receiver, the interference from other virtual users and the information spread into other dimensions are both ignored and only the received signal on the desired subcarrier, namely Y_k for virtual user k, is used for detection. Equivalently, the filter is given by $\mathbf{v}_k = H_k \mathbf{1}_k$, where $\mathbf{1}_k$ is an N-dimensional column vector, in which only the kth element is nonzero and equals 1.

B.2 Matched Filter

The MF filter, which is used in most practical CDMA receivers, regards the ICI as Gaussian noise. For virtual user k, $\mathbf{v}_k$ is simply $\mathbf{s}_k$. The output of the MF filter for virtual user k is given by

$$z_k = \mathbf{s}_k^H \mathbf{Y}. \quad (14)$$

B.3 LMMSE Detector

We can apply LMMSE multiuser detection [7], [10] to the equivalent CDMA system. The LMMSE detector is given by

$$\mathbf{v}_k = \mathbf{S}\left(\sigma_n^2 \mathbf{I} + \mathbf{R}\right)^{-1} \mathbf{1}_k. \quad (15)$$

The output of the LMMSE detector for user k is given by

$$z_k = \left(\left(\sigma_n^2\mathbf{I}+\mathbf{R}\right)^{-1}\mathbf{S}^H\mathbf{Y}\right)_k \tag{16}$$

where $\mathbf{R} \triangleq \mathbf{S}^H\mathbf{S}$ is the correlation matrix of the spreading codes for the different users. The filter output z_k is used for further detection. It is easy to verify that, for the LMMSE detector, the output signal-to-interference-plus-noise-ratio (SINR) of user k is given by

$$\mathrm{SINR}_k = \frac{1}{\left(\mathbf{I}+\frac{\mathbf{R}}{\sigma_n^2}\right)^+_{kk}} - 1 \tag{17}$$

where for matrix $\mathbf{A}$, $\mathbf{A}^+_{kk} \triangleq \left(\mathbf{A}^{-1}\right)_{kk}$[7].

C. Performance Measure

In traditional CDMA systems, when the received channel symbol power of user k equals 1, ME, which measures the impact of MAI and the efficiency of multiuser detection, is defined as

$$\eta_k \triangleq \frac{\mathrm{SINR}_k}{\frac{1}{\sigma_n^2}}. \tag{18}$$

Obviously, the larger η_k is, the more efficient the multiuser detection is. When η_k tends to 1, the impact of MAI vanlishes.

AME is defined as the limit of ME as $\sigma_n^2 \to 0$, namely

$$\bar{\eta}_k \triangleq \lim_{\sigma_n^2\to 0}\eta_k, \tag{19}$$

which measures the power efficiency when the performance is dominated by MAI. It is shown in [7] that, for the LMMSE detector, the AME is determined by the correlation matrix, which is given by

$$\bar{\eta}_k = \frac{1}{\mathbf{R}^+_{kk}}. \tag{20}$$

Similarly, we can define the ME for the equivalent CDMA system of an OFDM system, which is given by

$$\eta_k \triangleq \frac{\mathrm{SINR}_k}{\frac{\sum_{l=0}^{L-1}\bar{g}^{(l)}}{\sigma_n^2}}. \tag{21}$$

Recall that $\bar{g}^{(l)}$ is the average channel power gain of path l. Note that $\sum_{l=0}^{L-1}\sum_{k=0}^{N-1}|H_k^{(l)}|^2 = N\sum_{l=0}^{L-1}\sum_{m=0}^{N-1}|h_m^{(l)}|^2 = N^2\sum_{l=0}^{L-1}\bar{g}^{(l)}$. Then, we have

$$\frac{\sum_{l=0}^{L-1}\bar{g}^{(l)}}{\sigma_n^2} = \frac{\frac{1}{N}\sum_{l=0}^{L-1}\sum_{k=0}^{N-1}\left|H_k^{(l)}\right|^2}{N\sigma_n^2}$$

where the numerator is the average power of received X_k and the denominator is the noise power on subcarrier k. When the channel is time-invariant, we have

$$\mathrm{SINR}_k = \frac{\frac{1}{N}|H_0|^2}{N\sigma_n^2},$$

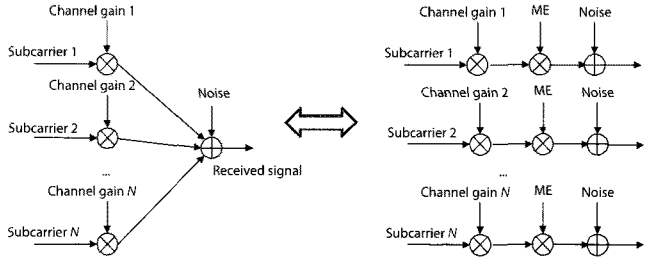

Fig. 1. Equivalence between multiple access channel and single-user channel.

which implies that $\eta_k = 1$.

Similarly, the corresponding AME is given by

$$\bar{\eta}_k = \frac{1}{\sum_{l=0}^{L-1}\bar{g}^{(l)}\mathbf{R}^+_{kk}}. \tag{22}$$

The concepts of ME and AME can be used to simplify the multiple access channel to multiple single-user channels. The equivalence is illustrated in Fig. 1. In the left hand side of the figure, the received signal is the sum of the signals from multiple subcarriers, which complicates the analysis. By employing the concepts of ME, the multiple access channel is decomposed into single-user channels by scaling the single-user signal with ME, as illustrated in the right hand side of Fig. 1, thus significantly simplifying the performance analysis. AME can further reduce the complexity of performance analysis when the system operates in the high SNR regime.

D. Discussion of Coded OFDM

It should be noted that we assume uncoded channel symbols in the OFDM system. Therefore, there is no redundancy to exploit. When the OFDM system is channel coded (COFDM), we can exploit the redundancy in the channel symbols to further improve the performance. Here we briefly discuss two approaches without further exploitation since it is beyond the scope of this paper.

D.1 Parallel Interference Cancelation

One approach is PIC [12], [14], which is more suitable for channel coding across different subcarriers. The above linear approach can be used in the first iteration. Then, the detection output will be used for channel decoding. The original ICI is reconstructed, according to the decoding output, and then fed back. The estimated ICI is canceled from the original signal and then put into the multiuser detection. The procedure iterates until the result converges.

D.2 Successive Interference Cancelation

Another approach is SIC [15], which is more suitable for the case in which channel coding is carried out in individual subcarriers. We can choose the the subcarrier having the strongest signal power. LMMSE detector can be used to decode the data over this subcarrier. Then, the ICI from this channel to other channels will be reconstructed and then canceled from the signals of other subcarriers. This ICI cancelation is carried out successively, in the order of descending signal power, until the last subcarrier.

IV. PERFORMANCE OF LINEAR DETECTORS WITH PERFECT CSI

In this section, we study the performance of linear multiuser detectors given the assumption that the CSI is perfectly known at the receiver. Although it is impossible to obtain perfect CSI in practical systems, this analysis provides performance bounds and insight for system design.

A. Frequency Flat Fading Channels

In this section, we consider the simplest case, a frequency flat channel, or equivalently, a single path channel ($L = 1$), and assume that the channel gains at each chip, $\{h_m^{(l)}\}_{l=0,\cdots,L-1,\, m=0,\cdots,N-1}$ are perfectly known. While simplifying the analysis, the analysis provides insight for each resolvable path and applies for channels having negligible time dispersion. We first provide the corresponding spreading codes and then compute the corresponding MEs and AMEs for the three types of linear detectors. Note that we ignore the path index l in all notations for simplicity.

A.1 Spreading Codes

Substituting $L = 1$ into (10), we obtain the spreading code matrix for the frequency flat fading case, which is given by

$$\mathbf{S} = \frac{1}{N}\begin{pmatrix} H_0 & H_{N-1} & \cdots & H_1 \\ H_1 & H_0 & \cdots & H_2 \\ \vdots & \vdots & \ddots & \vdots \\ H_{N-1} & H_{N-2} & \cdots & H_0 \end{pmatrix}. \tag{23}$$

It is easy to observe that, when $L = 1$, $\mathbf{S}$ is a circulant matrix. The following lemma provides a decomposition of the spreading code matrix $\mathbf{S}$ based on the circular matrix structure of $\mathbf{S}$:

Lemma 1: $\mathbf{S}$ can be decomposed as

$$\mathbf{S} = \mathbf{U}^{-1}\mathbf{\Lambda}\mathbf{U} \tag{24}$$

where

$$\mathbf{U} = \begin{pmatrix} 1 & 1 & \cdots & 1 \\ 1 & w & \cdots & w^{N-1} \\ \vdots & \vdots & \ddots & \vdots \\ 1 & w^{N-1} & \cdots & w^{(N-1)^2} \end{pmatrix} \tag{25}$$

and

$$\mathbf{\Lambda} = \begin{pmatrix} h_0 & 0 & \cdots & 0 \\ 0 & h_1 & \cdots & 0 \\ \vdots & \vdots & \ddots & \vdots \\ 0 & 0 & \cdots & h_{N-1} \end{pmatrix}. \tag{26}$$

The following lemma provides the properties of the above matrix decomposition, which will be used frequently later.

Lemma 2: The following properties of $\mathbf{S}$ hold:

$$\mathbf{U}^H\mathbf{U} = \mathbf{U}\mathbf{U}^H = N\mathbf{I}, \tag{27}$$

$$\mathbf{U}^{-1} = \frac{1}{N}\mathbf{U}^H, \text{ and } \left(\mathbf{U}^H\right)^{-1} = \frac{1}{N}\mathbf{U}, \tag{28}$$

$$\mathbf{U}\mathbf{s}_k = \left(h_0 \quad h_1 w^{-(k-1)} \quad \cdots \quad h_{N-1}w^{-(k-1)(N-1)}\right)^T. \tag{29}$$

- The DFT of the diagonal elements in matrix $\mathbf{\Lambda}$ is the first column of matrix $\mathbf{S}$, namely

$$\mathbf{U}^{-1}\mathbf{h} = \mathbf{s}_1 \tag{30}$$

where $\mathbf{h} = (h_0 \quad \cdots \quad h_{N-1})^T$.

A.2 Traditional Filter

The following proposition gives the ME of TF. The proof is given in Appendix I.

Proposition 1: The ME of TF is given by

$$\eta = \frac{|\bar{h}|^2\sigma_n^2}{\bar{g}\left(\sigma_n^2 + \sigma_h^2\right)} \tag{31}$$

Remark 1: From (31), we conclude that $\bar{\eta}_k = 0$, which means that the TF is very inefficient in the high SNR regime.

A.3 Matched Filter

The following proposition provides two expressions for the ME of MF. The proof is given in Appendix II.

Proposition 2: For MF, the ME is given by

$$\eta_k = \frac{1}{1 + \dfrac{(\kappa-1)\bar{g}}{\sigma_n^2}} = \frac{1}{1 + \dfrac{\sigma_g^2\bar{g}}{\sigma_n^2}} \tag{32}$$

where κ is the kurtosis of sequence $\{h_m\}_{m=0,\cdots,N-1}$ (recall that σ_g^2 is defined in (3)).

Remark 2: For MF, η_k is determined by the normalized variance of the channel power gain or the peakiness of the channel gain (note that the kurtosis of a random variable represents its peakiness). Again, we find that $\bar{\eta}_k = 0$, which means that MF is not an efficient detector in the high SNR regime.

A.4 LMMSE Filter

Applying the decomposition in (24), we have

$$\begin{aligned}\left(\mathbf{I} + \frac{\mathbf{R}}{\sigma_n^2}\right)^{-1} &= \left(\mathbf{I} + \frac{\mathbf{S}^H\mathbf{S}}{\sigma_n^2}\right)^{-1} \\ &= \mathbf{U}^{-1}\left(\mathbf{I} + \frac{\Lambda^*\Lambda}{\sigma_n^2}\right)^{-1}\mathbf{U} \\ &= \mathbf{U}^{-1}\begin{pmatrix} 1+\frac{|h_0|^2}{\sigma_n^2} & 0 & \cdots & 0 \\ 0 & 1+\frac{|h_1|^2}{\sigma_n^2} & \cdots & 0 \\ \vdots & \vdots & \ddots & \vdots \\ 0 & 0 & \cdots & 1+\frac{|h_{N-1}|^2}{\sigma_n^2} \end{pmatrix}\mathbf{U}.\end{aligned} \tag{33}$$

Applying the DFT relationship between the diagonal elements in $\mathbf{\Lambda}$ and the first column of $\mathbf{S}$ in Lemma 2, we have

$$\left(\mathbf{I} + \frac{\mathbf{R}}{\sigma_n^2}\right)_{kk}^{+} = \sum_{k=0}^{N-1}\left(1 + \frac{|h_k|^2}{\sigma_n^2}\right), \tag{34}$$

which is identical for all users. Therefore, all users in LMMSE detection share the same SINR, ME and AME in frequency flat channels. For simplicity, we ignore the user index k in the following discussion.

Then, the output SINR of the linear MMSE multiuser filter is given by

$$\mathrm{SINR} = \frac{N}{\sum_{k=0}^{N-1}\left(1+\frac{|h_k|^2}{\sigma_n^2}\right)^{-1}} - 1. \tag{35}$$

Based on (35), we obtain the ME in the following proposition:

Proposition 3: For the LMMSE multiuser detector, the ME is given by

$$\eta = \frac{N\sigma_n^2\left(\frac{N}{\sum_{k=0}^{N-1}\left(1+\frac{|h_k|^2}{\sigma_n^2}\right)^{-1}} - 1\right)}{\sum_{k=0}^{N-1}|h_k|^2}. \tag{36}$$

Consequently, we can obtain the AME in the following corollary:

Corollary 1: For the LMMSE multiuser detector, the AME is given by

$$\bar{\eta} = \frac{\frac{N^2}{\sum_{k=0}^{N-1}\frac{1}{|h_k|^2}}}{\sum_{k=0}^{N-1}|h_k|^2}. \tag{37}$$

Remark 3: An interesting observation from (37) is that the AME equals the ratio of the harmonic and arithmetic means of the channel gains, which is always less than or equal to 1. It is easy to check that, when the system is time invariant, namely $h_k = h$, $\forall k$, $\mathrm{SINR}_k = |h|^2/\sigma_n^2$ and $\eta = 1$, which means that ICI does not exist.

Remark 4: We can further simplify (37) in the case of slow fading channels, which is a reasonable assumption since it is difficult to estimate the channel gains and carry out coherent communication for fast fading channels. Then, we have

$$\begin{aligned}\bar{\eta} &= \frac{\frac{N}{\sum_{m=0}^{N-1}\frac{1}{\bar{g}+\delta g_m}}}{\bar{g}} \\ &= \frac{\frac{N}{\frac{1}{\bar{g}}\sum_{m=0}^{N-1}\frac{1}{1+\frac{\delta g_m}{\bar{g}}}}}{\bar{g}} \\ &= \frac{N}{\sum_{m=0}^{N-1}\sum_{k=0}^{\infty}\left(-\frac{\delta g_m}{\bar{g}}\right)^k} \\ &\approx \frac{N}{\sum_{m=0}^{N-1}\left(1-\frac{\delta g_m}{\bar{g}}+\left(\frac{\delta g_m}{\bar{g}}\right)^2\right)} \\ &= \frac{1}{1+\sigma_g^2},\end{aligned} \tag{38}$$

which is determined by the normalized variance of the channel power gain σ_g^2.

B. Frequency Selective Fading Channels

For frequency selective fading channels, $L > 1$, the spreading code matrix $\mathbf{S}$ is no longer a circulant matrix, thus losing the structure of decomposition in (24). It is also easy to verify that the eigenvectors of $\mathbf{S}_0$ are different from those of $\mathbf{S}_l$, $\forall l > 0$ (note that $\mathbf{S}_l$ is defined as the spreading code generated by the lth path). The analysis for the TF and MF is similar to that for the frequency flat case. For the LMMSE filter, it is difficult to obtain explicit expressions for evaluating the performance of multiuser detection in frequency selective fading channels. However, we can consider a scenario in which there exist two resolvable paths and the channel power gain for the second path is sufficiently small relative to that for the first path. Then, we can analyze the performance by considering the signal along the second path as a perturbation of that for the first path. We also assume slow fading, similar to the analysis in (38). For simplicity, we consider only the AME, which is determined by the diagonal elements of $\mathbf{R}^{-1}$.

Suppose the spreading code matrix is given by the following form:

$$\mathbf{S} = \mathbf{S}_0 + t\mathbf{S}_1 \tag{39}$$

where $\mathbf{S}_0$ is the spreading code generated by the first path, which is given in (23), $\mathbf{S}_1$ is that of the second path, which is scaled by $1/t$ and the elements are given by

$$(\mathbf{S}_1)_{pq} = \frac{1}{tN}H^{(1)}_{\mathrm{mod}(p-q,N)}w^{-\tau_1(q-1)},$$

and t is a sufficiently small real number which is given by

$$t = \frac{\sum_{k=0}^{N-1}|H_k^1|^2}{\sum_{k=0}^{N-1}|H_k^0|^2}.$$

Then, we can obtain the following proposition, whose proof is given in Appendix III:

Proposition 4: For $L = 2$, with sufficiently slow fading and sufficiently small t in (39), compared with the frequency flat channels, we have

- if the phase difference between $h_0^{(0)}$ and $h_0^{(1)}$ lies in $\left[-\frac{\pi}{2}, \frac{\pi}{2}\right]$, the AME is decreased;
- if the phase difference between $h_0^{(0)}$ and $h_0^{(1)}$ lies in $\left[\frac{\pi}{2}, \frac{3\pi}{2}\right]$, the AME is increased.

Remark 5: Therefore, whether an additional resolvable path increases the AME is determined by the phase difference of the two paths. Since the phase difference is uniformly distributed, the additional path benefits or impairs the AME equiprobably.

V. LINEAR DETECTORS WITHOUT CSI

In the previous section, we assume that perfect CSI is available at the receiver. However, in practical systems, the channel estimation is imperfect due to the existence of thermal noise and interference. Even when thermal noise or interference does not exist, the channel estimate is still imperfect, except for the impractical case that all data symbols are known at the receiver

(in this situation, no information is conveyed), since the channel parameters are random variables and time-varying. The channel estimation error will degrade the performance since the designed multiuser detector is mismatched.

A. Truncated Spreading Codes

In practical systems, the spreading codes of the virtual users are unknown to the receiver, which requires pilots, namely training data, for channel estimation in the frequency domain. In TF, only the diagonal elements in matrix $\mathbf{S}$ are unknown. This can be estimated from the pilots sent on certain subcarriers. However, both MF and LMMSE filters need to estimate the entire $N \times N$ matrix $\mathbf{S}$, which requires prohibitive numbers of pilots when N is large (e.g., in WiMax system, $N = 1024$). Moreover, in LMMSE filters, the inversion of an $N \times N$ matrix is needed for each OFDM symbol and causes substantial computational cost.

An intuitive approach to tackle the prohibitive amount of pilots and computational overhead is to truncate the spreading code to a much shorter length. As will be demonstrated using numerical results, most of the power of a symbol on a subcarrier is confined to this subcarrier and its two adjacent subcarriers. Therefore, we can assume that $\mathbf{S}$ is a band matrix such that $\mathbf{S}_{pq} = 0$, if $|p - q| > 1$. We call the columns of matrix $\mathbf{S}$ *truncated spreading codes*. Such an approximation can substantially reduce the number of unknowns in $\mathbf{S}$. It is easy to verify that $\mathbf{R} = \mathbf{S}^H\mathbf{S}$ is a also a band matrix; hence the inversion of the band matrix can substantially reduce the computational cost.

B. Estimating Truncated Spreading Codes

For simplicity, we assume that the number of paths, L, and the corresponding delays, $\{\tau_l\}_{l=0,\cdots,L-1}$, are known. When truncated spreading codes are used, there exist $3L$ unknowns in $\mathbf{S}$, namely $\left\{H_0^{(l)}\right\}_{l=0,\cdots,L-1}$, $\left\{H_1^{(l)}\right\}_{l=0,\cdots,L-1}$, and $\left\{H_{N-1}^{(l)}\right\}_{l=0,\cdots,L-1}$.

We place pilot symbols, which are known to both the transmitter and receiver, on P clusters, each of which consists of three consecutive subcarriers (accordingly, there exist $3P$ pilot subcarriers). The index of the center subcarrier of the ith cluster is denoted by p_i. Then, when there are no thermal noise and ICI from the subcarriers conveying information symbols, which are at least one subcarrier away, the output signal at subcarrier p_i is given by

$$Y_{p_i} = \sum_{l=0}^{L-1} H_0^{(l)} w^{-\tau_l p_i} X_{p_i} + \sum_{l=0}^{L-1} H_{N-1}^{(l)} w^{-\tau_l (p_i+1)} X_{p_i+1} + \sum_{l=0}^{L-1} H_1^{(l)} w^{-\tau_l (p_i-1)} X_{p_i-1}.$$

Collecting the P equations into a vector form, we have

$$\mathbf{X}_0\mathbf{H}_0 + \mathbf{X}_{N-1}\mathbf{H}_1 + \mathbf{X}_1\mathbf{H}_{N-1} = \mathbf{Y}_T \tag{40}$$

where

$$\begin{aligned}
\mathbf{Y}_T &= (Y_{p_1}, \cdots, Y_{p_P})^T, \\
(\mathbf{X}_0)_{rs} &= X_{p_r} w^{-\tau_{s-1}(p_r)}, \quad r = 1, \cdots, P, s = 1, \cdots, L, \\
(\mathbf{X}_{N-1})_{rs} &= X_{p_r+1} w^{-\tau_{s-1}(p_r+1)}, \quad r = 1, \cdots, P, s = 1, \cdots, L, \\
(\mathbf{X}_1)_{rs} &= X_{p_r-1} w^{-\tau_{s-1}(p_r-1)}, \quad r = 1, \cdots, P, s = 1, \cdots, L, \\
\mathbf{H}_0 &= \left(H_0^{(0)} \ \cdots \ H_0^{(L-1)}\right)^T, \\
\mathbf{H}_{N-1} &= \left(H_{N-1}^{(0)} \ \cdots \ H_{N-1}^{(L-1)}\right)^T, \\
\mathbf{H}_1 &= \left(H_1^{(0)} \ \cdots \ H_1^{(L-1)}\right)^T
\end{aligned}$$

and

$$\mathbf{H}_1 = \left(H_1^{(0)} \ \cdots \ H_1^{(L-1)}\right)^T.$$

We can further simplify (40) to

$$\mathbf{X}_T\mathbf{H} = \mathbf{Y}_T \tag{41}$$

where subscript T denotes training and $\mathbf{X}_T = (\mathbf{X}_0, \mathbf{X}_{N-1}, \mathbf{X}_1)$, and $\mathbf{H} = (\mathbf{H}_0^H, \mathbf{H}_1^H, \mathbf{H}_{N-1}^H)^H$.

If the rank of $\mathbf{X}_T$ is equal to $3L$, $\mathbf{H}$ is uniquely determined by $\mathbf{X}_T$ and $\mathbf{Y}_T$. Therefore, it is required that $P \geq 3L$. As will be demonstrated using numerical results, by choosing the pilot symbols in $\mathbf{X}_T$ randomly, the rank of $\mathbf{X}_T$ equals $3L$ with large probability, when $P \geq 3L$.

VI. NUMERICAL RESULTS

In this section, we provide simulation results to validate the analytical results derived in the previous sections. Note that the expectations and standard deviations of MEs in Figs. 4 and 6 are listed in Table 1.

A. System Configurations

In our numerical simulation, we adopt the following configuration for the OFDM system:

- 512 subcarriers ($N = 512$);
- OFDM symbol period $T_s = 0.1$ ms;
- carrier frequency: 5 GHz;
- we primarily focus on frequency flat fading ($L = 1$); for the multipath case, we assume $L = 2$ and the average powers of the two paths are 0.9 and 0.1, respectively; the corresponding path delays are 0 and 50 OFDM chips, respectively.

Jakes model [16] is adopted to generate the time-varying fading process. The detailed procedure for generating the fading process is given in [17]. We assume that

- the receiver is a mobile station and its speed is 100 km/hour, unless noted otherwise;
- there is no line-of-sight (LOS) path and the channel gain amplitude is Rayleigh distributed;

B. Channel Variation

Fig. 2 shows the cumulative distribution function (CDF) of the variance of the channel power gain (normalized by the square of the average channel power gain) within one OFDM

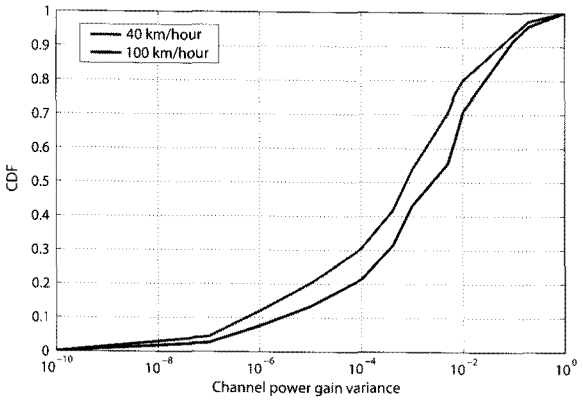

Fig. 2. CDF of channel power gain variance.

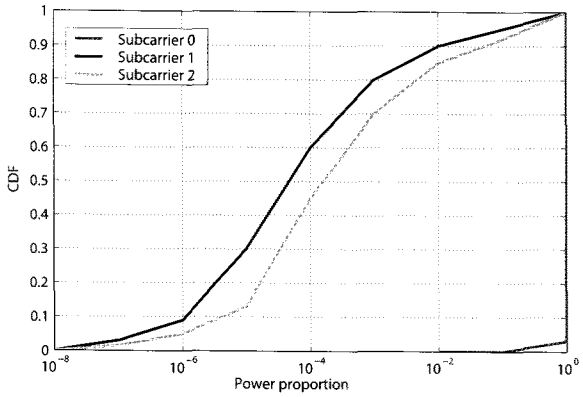

Fig. 3. CDF of the proportion of the power of X_0 in subcarriers 0, 1, and 2.

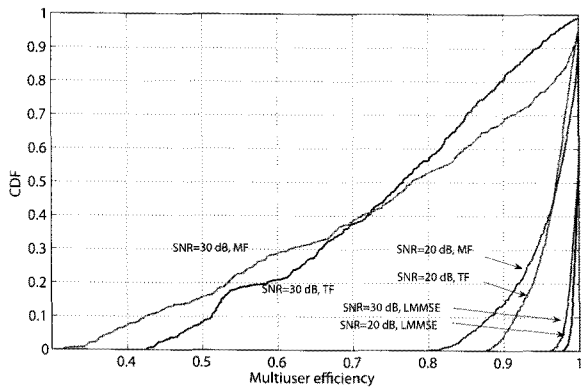

Fig. 4. CDF of ME in frequency flat fading channels.

symbol. In the simulation, the mobile station speed equals 40 km/hour or 100 km/hour. We can observe that the channel varies much faster in the high mobility scenario (100 km/hour). In the moderate speed (40 km/hour) case, the channel variance within one OFDM symbol is small, which implies that the ICI is negligible.

C. Power Dispersion in Frequency Domain

Fig. 3 shows the CDF of the proportion of the power of X_0 contained in subcarriers 0, 1, and 2 at the channel output. We can observe that most of the power is contained in subcarriers 0 and 1. This demonstrates the validity of the truncated spreading code in subsection V-B.

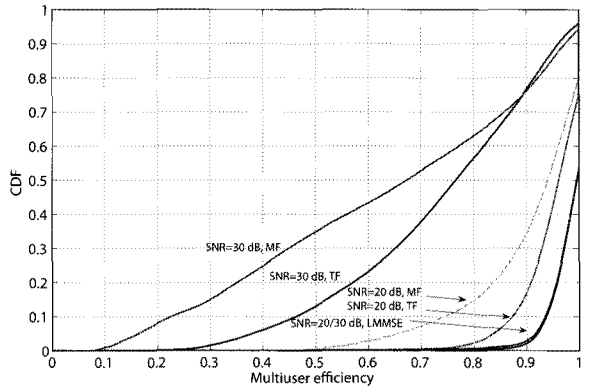

Fig. 5. CDF of ME in frequency flat selective channels.

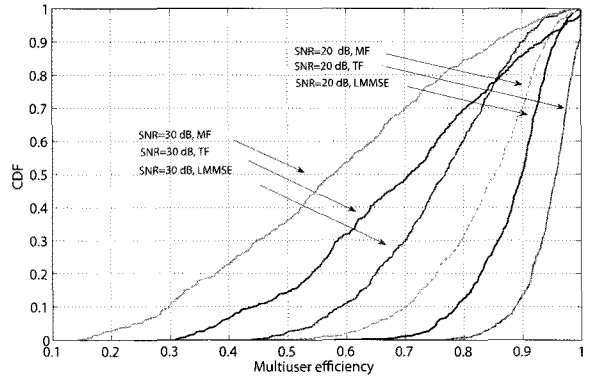

Fig. 6. CDF of ME in frequency flat fading channels with truncated spreading codes.

D. Performance with Perfect CSI

Fig. 4 shows the CDF curves of ME given the assumptions of frequency flat channels and perfect CSI. We tested the cases of SNR $=$ 20 dB and SNR $=$ 30 dB. Note that the two CDF curves for the LMMSE detector almost coincide. We can observe that LMMSE detector achieves considerably higher ME than MF and TF, particularly when SNR $=$ 30 dB. MF partially outperforms TF when the ME is close to 1.

Fig. 5 shows the CDF curves of ME given the assumptions of frequency selective channels and perfect CSI. We can draw similar conclusions as those from Fig. 4. However, the gap between the LMMSE detector and TF/MF is smaller in frequency selective channels than in frequency flat channels and the range of ME is larger since different virtual users may receive different powers due to frequency selectivity.

E. Performance with Imperfect CSI

Fig. 6 shows the CDF curves of ME when the receiver uses the estimated truncated spreading code, which is proposed in subsection V-B. The simulation is based on a frequency flat fading channel, whose configuration is the same as that in Fig. 4, and $P = 20$ (recall that P denotes the number of pilot clusters), where the pilots occupy 60 subcarriers and incur a roughly 12% overhead for frequency spectrum usage. We can observe that the LMMSE detector achieves more robust performance than TF when SNR $=$ 30 dB and the corresponding ME is roughly lower bounded by 0.5.

Table 1. Expectation and standard deviation of ME in Difference Scenarios: Frequency flat channel (FFC), frequency selective channel (FSC), and truncated spreading code (TSC).

Scenario	SNR	Algorithm	Expectation	Deviation
FFC	30 dB	MF	0.7479	0.2059
FFC	30 dB	TF	0.7451	0.1577
FFC	30 dB	LMMSE	0.9941	0.0078
FFC	20 dB	MF	0.9558	0.0462
FFC	20 dB	TF	0.9625	0.0297
FFC	20 dB	LMMSE	0.9966	0.0044
FSC	30 dB	MF	0.6353	0.2747
FSC	30 dB	TF	0.7383	0.1867
FSC	30 dB	LMMSE	0.9769	0.0423
FSC	20 dB	MF	0.9046	0.1102
FSC	20 dB	TF	0.9472	0.0614
FSC	20 dB	LMMSE	0.9791	0.0312
TSC	30 dB	MF	0.5766	0.2050
TSC	30 dB	TF	0.6963	0.1762
TSC	30 dB	LMMSE	0.7567	0.1164
TSC	20 dB	MF	0.8354	0.0954
TSC	20 dB	TF	0.9479	0.0433
TSC	20 dB	LMMSE	0.8842	0.0652

VII. CONCLUSIONS

In this paper, we have applied the technique of multiuser detection in CDMA systems to mitigate the ICI in OFDM systems, which is caused by time-varying fading channels. Three multiuser detectors, namely TF, MF, and LMMSE detectors, have been analyzed. The performance, measured using ME and AME, has been analyzed for both frequency flat and frequency selective fading channels given the assumption that the CSI is known. For the case of unknown CSI, which is more reasonable in practical systems, the performance has been analyzed for unbiased time domain channel estimation errors. An algorithm using an estimated truncated spreading code has been proposed. Numerical results show that the LMMSE detector achieves the best performance in the high SNR regime when CSI is known. When an unbiased channel estimation error exists, the LMMSE detector still attains the most robust performance when the SNR is sufficiently large and channel variation is large. Numerical results also show that, by using our estimated truncated spreading code, the LMMSE detector attains more robust performance than both TF and MF detectors.

APPENDICES

I. PROOF OF PROPOSITION 1

Proof: It is easy to verify that the output SINR of TF is given by

$$\begin{aligned}\mathrm{SINR}_k &= \frac{N\left\|\mathbf{S}_{kk}\right\|^2}{N\sigma_n^2 + N\sum_{i\neq k}\left\|\mathbf{S}_{ki}\right\|^2} \\ &= \frac{\left|H_0\right|^2}{N^2\sigma_n^2 + \sum_{k=1}^{N-1}\left|H_k\right|^2}.\end{aligned} \tag{42}$$

According to the property of the DFT, we know $|H_0|^2 = N^2|\bar{h}|^2$. We also have

$$\begin{aligned}\sum_{k=1}^{N-1}|H_k|^2 &= \sum_{k=0}^{N-1}|H_k|^2 - |H_0|^2 \\ &= N\sum_{k=0}^{N-1}|h_k|^2 - N^2|\bar{h}|^2 \\ &= N^2(\bar{g} - |\bar{h}|^2) \\ &= N^2\sigma_h^2.\end{aligned} \tag{43}$$

Substituting (43) into (42), we can obtain the conclusion. □

II. PROOF OF PROPOSITION 2

Proof: It is easy to verify that the output SINR of MF is given by

$$\mathrm{SINR}_k = \frac{\left\|\mathbf{s}_k\right\|^4}{\left\|\mathbf{s}_k\right\|^2\sigma_n^2 + \sum_{i\neq k}\left\|\mathbf{s}_k^H\mathbf{s}_i\right\|^2} \tag{44}$$

where $\|\mathbf{s}_k\|^4 = \left|\mathbf{s}_k^H\mathbf{s}_k\right|^2$.

To further simplify (44), we have

$$\begin{aligned}\left\|\mathbf{s}_k\right\|^4 &= \left(\mathbf{s}_k^H\mathbf{s}_k\right)^2 \\ &= \left(\frac{1}{N^2}\sum_{m=0}^{N-1}|H_m|^2\right)^2 \\ &= \left(\frac{1}{N}\sum_{m=0}^{N-1}|h_m|^2\right)^2 \\ &= \bar{g}^2\end{aligned} \tag{45}$$

where the third equation is due to Parseval's equality for the DFT.

For the denominator in (44), we have

$$\begin{aligned}\left\|\mathbf{s}_k\right\|^2 &= \mathbf{s}_k^H\mathbf{s}_k \\ &= \frac{1}{N^2}\sum_{m=0}^{N-1}|H_m|^2 \\ &= \frac{1}{N}\sum_{m=0}^{N-1}|h_m|^2 \\ &= \bar{g}\end{aligned} \tag{46}$$

and

$$\begin{aligned}\sum_{i\neq k}\left\|\mathbf{s}_k^H\mathbf{s}_i\right\|^2 &= \sum_{i=0}^{N-1}\left|\mathbf{s}_k^H\mathbf{s}_i\right|^2 - \left\|\mathbf{s}_k\right\|^4 \\ &= \mathbf{s}_k^H\left(\sum_{i=0}^{N-1}\mathbf{s}_i\mathbf{s}_i^H\right)\mathbf{s}_k - \left\|\mathbf{s}_k\right\|^4 \\ &= \mathbf{s}_k^H\mathbf{S}\mathbf{S}^H\mathbf{s}_k - \left\|\mathbf{s}_k\right\|^4 \\ &= \mathbf{s}_k^H\mathbf{U}^{-1}\mathbf{\Lambda}\mathbf{\Lambda}^*\mathbf{U}\mathbf{s}_k - \left\|\mathbf{s}_k\right\|^4 \\ &= \frac{1}{N}\sum_{m=0}^{N-1}|h_m|^4 - \left(\frac{1}{N}\sum_{m=0}^{N-1}|h_m|^2\right)^2\end{aligned}$$

where the last equation uses (29).

Then (44) can be rewritten as

$$\begin{aligned}\mathrm{SINR}_k &= \frac{1}{\frac{N\sigma_n^2}{\sum_{m=0}^{N-1}|h_m|^2}+\frac{N\sum_{m=0}^{N-1}|h_m|^4}{\left(\sum_{m=0}^{N-1}|h_m|^2\right)^2}-1} \\ &= \frac{1}{\frac{\sigma_n^2}{\bar{g}}+\kappa-1}. \end{aligned} \quad (47)$$

Recall that κ is the kurtosis of sequence $\{h_m\}_{m=0,\cdots,N-1}$, which measures the peakiness of a random variable.

Then, it is easy to verify that $\sigma_g^2=\kappa-1$ which represents the variance of the channel power gains and (47) is equal to

$$\mathrm{SINR}_k = \frac{1}{\frac{\sigma_n^2}{\bar{g}}+\sigma_g^2}. \quad (48)$$

The conclusion of the proposition is then obtained from the above two equations. □

III. PROOF OF PROPOSITION 3

Proof: The covariance matrix $\mathbf{R}=\mathbf{S}^H\mathbf{S}$ is a function of t and we denote it by $\mathbf{R}(t)$. Then, we have

$$\mathbf{R}(t)=\mathbf{S}_1^H\mathbf{S}_1+t\left(\mathbf{S}_1^H\mathbf{S}_2+\mathbf{S}_2^H\mathbf{S}_1\right)+t^2\mathbf{S}_2^H\mathbf{S}_2 \quad (49)$$

and

$$\left.\frac{d\mathbf{R}(t)}{dt}\right|_{t=0}=\mathbf{S}_1^H\mathbf{S}_2+\mathbf{S}_2^H\mathbf{S}_1.$$

By differentiating the inverse matrix, we have

$$\mathbf{R}^{-1}(t)=\mathbf{R}^{-1}(0)-\mathbf{R}^{-1}(0)\left.\frac{d\mathbf{R}(t)}{dt}\right|_{t=0}\mathbf{R}^{-1}(0)+o(t) \quad (50)$$

where

$$\begin{aligned}&\mathbf{R}^{-1}(0)\left.\frac{d\mathbf{R}(t)}{dt}\right|_{t=0}\mathbf{R}^{-1}(0) \\ &=\left(\mathbf{S}_1^H\mathbf{S}_1\right)^{-1}\left(\mathbf{S}_1^H\mathbf{S}_2+\mathbf{S}_2^H\mathbf{S}_1\right)\left(\mathbf{S}_1^H\mathbf{S}_1\right)^{-1} \\ &=\left(\mathbf{U}^H\mathbf{\Lambda}^*\left(\mathbf{U}^{-1}\right)^H\mathbf{U}^{-1}\mathbf{\Lambda}\mathbf{U}\right)^{-1} \\ &\quad\cdot\left(\mathbf{S}_1^H\mathbf{S}_2+\mathbf{S}_2^H\mathbf{S}_1\right)\left(\mathbf{U}^H\mathbf{\Lambda}^*\left(\mathbf{U}^{-1}\right)^H\mathbf{U}^{-1}\mathbf{\Lambda}\mathbf{U}\right)^{-1} \\ &=\left(\frac{1}{N}\mathbf{U}^H\mathbf{\Lambda}^*\mathbf{\Lambda}\mathbf{U}\right)^{-1}\left(\mathbf{S}_1^H\mathbf{S}_2+\mathbf{S}_2^H\mathbf{S}_1\right)\left(\frac{1}{N}\mathbf{U}^H\mathbf{\Lambda}^*\mathbf{\Lambda}\mathbf{U}\right)^{-1} \\ &=\mathbf{U}^{-1}\left(\mathbf{\Lambda}^*\mathbf{\Lambda}\right)^{-1}\mathbf{U}\left(\mathbf{U}^H\mathbf{\Lambda}^*\left(\mathbf{U}^{-1}\right)^H\mathbf{S}_2+\mathbf{S}_2^H\mathbf{U}^{-1}\mathbf{\Lambda}\mathbf{U}\right) \\ &\quad\cdot\mathbf{U}^{-1}\left(\mathbf{\Lambda}^*\mathbf{\Lambda}\right)^{-1}\mathbf{U} \\ &=\mathbf{U}^{-1}\mathbf{\Lambda}^{-1}\mathbf{U}\mathbf{S}_2\mathbf{U}^{-1}\left(\mathbf{\Lambda}^*\mathbf{\Lambda}\right)^{-1}\mathbf{U}+\mathbf{U}^{-1}\left(\mathbf{\Lambda}^*\mathbf{\Lambda}\right)^{-1}\mathbf{U}\mathbf{S}_2^H \\ &\quad\cdot\mathbf{U}^{-1}\left(\mathbf{\Lambda}^*\right)^{-1}\mathbf{U}.\end{aligned}$$

For sufficiently small t, we can ignore the small order term $o(t)$ in (50). Then, the diagonal elements in the linear term in (50) represent the perturbation of the second path. It is easy to verify that

$$\begin{aligned}&\mathbf{U}^{-1}\mathbf{\Lambda}^{-1}\mathbf{U}\mathbf{S}_2\mathbf{U}^{-1}\left(\mathbf{\Lambda}^*\mathbf{\Lambda}\right)^{-1}\mathbf{U} \\ &=\left(\mathbf{U}^{-1}\left(\mathbf{\Lambda}^*\mathbf{\Lambda}\right)^{-1}\mathbf{U}\mathbf{S}_2^H\mathbf{U}^{-1}\left(\mathbf{\Lambda}^*\right)^{-1}\mathbf{U}\right)^H\end{aligned}$$

Therefore, we have

$$\begin{aligned}&\left(\mathbf{R}^{-1}(0)\left.\frac{d\mathbf{R}(t)}{dt}\right|_{t=0}\mathbf{R}^{-1}(0)\right)_{kk} \\ &=2\mathrm{Re}\left(\mathbf{U}^{-1}\mathbf{\Lambda}^{-1}\mathbf{U}\mathbf{S}_2\mathbf{U}^{-1}\left(\mathbf{\Lambda}^*\mathbf{\Lambda}\right)^{-1}\mathbf{U}\right)_{kk}. \end{aligned} \quad (51)$$

It is easy to check that $\mathbf{U}^{-1}\mathbf{\Lambda}^{-1}\mathbf{U}$ is a cyclic matrix, in which the elements are the DFT of sequence $\left\{1/h_n^{(0)}\right\}_{n=0,\cdots,N-1}$ and $\mathbf{U}^{-1}\left(\mathbf{\Lambda}^*\mathbf{\Lambda}\right)^{-1}\mathbf{U}$ is also a cyclic matrix, in which the elements are the DFT of sequence $\left\{1/\left|h_n^{(0)}\right|^2\right\}_{n=0,\cdots,N-1}$. Particularly, the diagonal elements of the above two matrices are the zero frequency components of the corresponding sequences and they dominate the matrix due to the slow fading assumption. Therefore, the diagonal elements in matrix $\mathbf{R}^{-1}(0)\left.\frac{d\mathbf{R}(t)}{dt}\right|_{t=0}\mathbf{R}^{-1}(0)$ are dominated by those of matrices $\mathbf{U}^{-1}\mathbf{\Lambda}^{-1}\mathbf{U}$, $\mathbf{S}_2$ and $\mathbf{U}^{-1}\left(\mathbf{\Lambda}^*\mathbf{\Lambda}\right)^{-1}\mathbf{U}$. Notice that the diagonal elements of $\mathbf{U}^{-1}\left(\mathbf{\Lambda}^*\mathbf{\Lambda}\right)^{-1}\mathbf{U}$ are positive; thus the signs of the diagonal elements in matrix $\mathbf{R}^{-1}(0)\left.\frac{d\mathbf{R}(t)}{dt}\right|_{t=0}\mathbf{R}^{-1}(0)$ are dominated by the phases of those in matrices $\mathbf{U}^{-1}\mathbf{\Lambda}^{-1}\mathbf{U}$ and $\mathbf{S}_2$.

Applying the slow fading assumption again, we can see that the zero frequency components of $\left\{1/h_n^{(0)}\right\}_{n=0,\cdots,N-1}$ and $\left\{h_n^{(1)}\right\}_{n=0,\cdots,N-1}$ are close to $1/h_0^{(0)}$ and $h_0^{(1)}$, respectively. Therefore, the signs of the diagonal elements in matrix $\mathbf{R}^{-1}(0)\left.\frac{d\mathbf{R}(t)}{dt}\right|_{t=0}\mathbf{R}^{-1}(0)$ are determined by the real part of $h_0^{(1)}/h_0^{(0)}$, which implies the conclusion. □

REFERENCES

[1] A. Stamoulis, S. N. Diggavi, and N. Al-Dhahir, "Intercarrier interference in MIMO OFDM," *IEEE Trans. Signal Process.*, vol. 50, pp. 2451–2464, Oct. 2002.

[2] Y. Mostofi and D. C. Cox, "ICI mitigation for pilot-aided OFDM mobile systems," *IEEE Trans. Wireless Commun.*, vol. 4, pp. 765–774, Mar. 2005.

[3] J. Armstrong, "Analysis of new and existing methods of reducing intercarrier interference due to carrier frequency offset in OFDM," *IEEE Trans. Commun.*, vol. 47, pp. 365–369, Mar. 1999.

[4] D. Marabissi, R. Fantacci, and S. Papini, "Robust multiuser interference cancellation for OFDM systems with frequency offset," *IEEE Trans. Wireless Commun.*, vol. 5, pp. 3068–3076, Nov. 2006.

[5] Y. Mostofi and D. C. Cox, "Timing synchronization in high mobility OFDM," in *Proc. IEEE ICC*, June 2004.

[6] D. Huang and K. B. Lataief, "Enhanced carrier frequency offset estimation for OFDM using channel side information," *IEEE Trans. Wireless Commun.*, vol. 5, pp. 2784–2793, Oct. 2006.

[7] S. Verdú, *Multiuser Detection.* Cambridge University Press, Cambridge, UK, 1998.

[8] S. Verdú, "Minimum probability of error for asynchronous Gaussian multiple-access channels," *IEEE Trans. Inf. Theory*, vol. 32, pp. 85–96, Jan. 1986.

[9] S. Verdú, *Optimal Multi-User Signal Detection.* Ph.D. thesis, University of Illinois at Urbana-Champaign, Aug. 1984.

[10] R. Lupas and S. Verdú, "Linear multiuser detectors for synchronous code-division multiple-acess channels," *IEEE Trans. Inf. Theory*, vol. 35, pp. 123–136, Aug. 1989.

[11] D. Tse and S. Hanly, "Linear multiuser receivers: Effective interference, effective bandwidth and user capacity," *IEEE Trans. Inf. Theory*, vol. 45, pp. 641–657, Mar. 1999.

[12] P. Alexander, A. Grant, and M. C. Reed, "Iterative detection of code-division multiple-acess with error control coding," *Eur. Trans. Telecommun.*, vol. 9, pp. 419–426, Aug. 1998.
[13] H. Li and H. V. Poor, "Power allocation and spectral efficiency of DS-CDMA systems in fading channels with fixed QoS—Part I: Single-rate case," *IEEE Trans. Wireless Commun.*, vol. 5, pp. 2516–2528, Sept. 2006.
[14] X. Wang and H. V. Poor, "Subspace methods for blind channel estimation and multiuser detection in CDMA systems," *Wireless Networks*, vol. 6, pp. 59–71, Feb. 2000.
[15] S. Shamai and S. Verdú, "Decoding only the strongest CDMA users," *Codes, Graphs, and Systems*, R. Blahut and R. Koetter, Eds., pp. 217–228, Kluwer, 2002.
[16] W. C. Jakes, *Mircrowave Mobile Communications*. IEEE Press, Piscataway, NJ, 1994.
[17] 3rd generation partnership project 2 (3GPP2), *cdma2000 evaluation methodology*, revision 0, Dec. 2004.

Husheng Li received the B.S. and M.S. degrees in electronic engineering from Tsinghua University, Beijing, China, in 1998 and 2000, respectively, and the Ph.D. degree in Electrical Engineering from Princeton University, Princeton, NJ, in 2005. From 2005 to 2007, he worked as a Senior Engineer at Qualcomm Inc., San Diego, CA. In 2007, he joined the EECS department of the University of Tennessee, Knoxville, TN, as an Assistant Professor. His research is mainly focused on statistical signal processing, wireless communications, networking, and smart grid. He is the Recipient of the Best Paper Award of EURASIP Journal of Wireless Communications and Networks, 2005 (together with his Ph.D. advisor: Prof. H. V. Poor).